

EUROPEAN ORGANIZATION FOR NUCLEAR RESEARCH  
Proposal to the ISOLDE and Neutron Time-of-Flight Committee

Measurement of  $^{28,29,30}\text{Si}(n, \gamma)$  capture cross sections to explain isotopic abundances in presolar grains

January 11, 2023

C. Lederer-Woods<sup>1</sup>, A. Mengoni<sup>2</sup>, J. Andrzejewski<sup>3</sup>, M. Boromiza<sup>4</sup>, A. Casanovas<sup>5</sup>, S. Cristallo<sup>6</sup>, M. Dietz<sup>7</sup>, C. Domingo-Pardo<sup>8</sup>, A. Gawlik-Ramiega<sup>3</sup>, G. Gervino<sup>9</sup>, A. Gugliemelli<sup>2</sup>, C. Gustavino<sup>10</sup>, T. Heftrich<sup>11</sup>, J. Lerendegui<sup>8</sup>, A. Manna<sup>12,13</sup>, C. Massimi<sup>12</sup>, A. Negret<sup>4</sup>, N. Patronis<sup>14</sup>, J. Perkowski<sup>3</sup>, C. Petrone<sup>4</sup>, M. Pignatari<sup>15</sup>, T. Rauscher<sup>16,17</sup>, R. Reifarh<sup>11</sup>, A. Rooney<sup>1</sup>, N. Sosnin<sup>1</sup>, O. Straniero<sup>6</sup>, S. Tosi<sup>18</sup>, P. Ventura<sup>19</sup>, D. Vescovi<sup>11</sup>, P.J. Woods<sup>1</sup> and the n\_TOF Collaboration

<sup>1</sup> School of Physics and Astronomy, University of Edinburgh, UK. <sup>2</sup> ENEA and INFN-Bologna, Italy. <sup>3</sup> University of Lodz, Poland. <sup>4</sup> IFIN-HH, Romania. <sup>5</sup> Universitat Politècnica Catalunya, Spain. <sup>6</sup> INAF - Osservatorio Astronomico d'Abruzzo, Teramo, Italy. <sup>7</sup> Physikalisch-Technische Bundesanstalt (PTB), Germany. <sup>8</sup> Univ. of Valencia and CSIC, Spain. <sup>9</sup> INFN, Sezione di Torino, Italy. <sup>10</sup> INFN, Sezione di Roma-1, Italy. <sup>11</sup> Goethe Universität Frankfurt, Germany. <sup>12</sup> Università Di Bologna, Italy. <sup>13</sup> CERN, Switzerland. <sup>14</sup> Department of Physics, University of Ioannina, 45110 Ioannina, Greece. <sup>15</sup> Konkoly Observatory, Hungary. <sup>16</sup> Department of Physics, University of Basel, Switzerland. <sup>17</sup> Centre for Astrophysics Research, University of Hertfordshire, UK. <sup>18</sup> Università Roma 3, Italy. <sup>19</sup> INAF - Osservatorio Astronomico di Roma, Italy.

**Spokespersons:** Claudia Lederer-Woods [claudia.lederer@ed.ac.uk]  
Alberto Mengoni [alberto.mengoni@cern.ch]

**Technical coordinator:** Oliver Aberle [oliver.aberle@cern.ch]

**Abstract:** Neutron capture reactions on the stable silicon isotopes  $^{28,29,30}\text{Si}$  are of key importance to understand the production of silicon in massive stars and isotopic abundances in presolar stardust grains. However, there are only few experimental data at astrophysical neutron energies, and results from previous measurements are discrepant. We propose to measure neutron capture cross sections on  $^{28,29,30}\text{Si}$  at EAR-1 and EAR-2, with the aim to obtain high accuracy data on neutron resonances, and at thermal neutron energies (25.3 meV), respectively.

**Requested protons:**  $7 \times 10^{18}$  (EAR-1) and  $1.1 \times 10^{18}$  (EAR-2) protons on target  
**Experimental Area:** EAR1 and EAR2



# 1 Introduction

The aim of this proposal is to determine accurate neutron capture cross sections on the stable silicon isotopes  $^{28,29,30}\text{Si}$ , to increase accuracy and resolve discrepancies between previous measurements. The most recent measurement of  $^{28,29,30}\text{Si}$  neutron capture cross sections was performed via the time-of-flight technique by Guber et al [1]. Maxwellian averaged cross sections were deduced from the measured resonance parameters combined with calculations of the direct capture component. For all isotopes, they found smaller stellar cross sections compared to previous data. Concerning the  $^{28}\text{Si}(n,\gamma)$  and  $^{29}\text{Si}(n,\gamma)$  cross sections, the only other data are more than 40 years old [2, 3] and while stellar cross sections for  $^{29}\text{Si}$  are agreeing with [1] within uncertainties, there is a factor of about 2 difference for  $^{28}\text{Si}$ . For the case of  $^{30}\text{Si}(n,\gamma)$ , the MACS in [1] was found to be almost 2 times smaller than results from an activation measurement by Beer *et al.* [4]. At present, the source of such a big difference for the  $^{30}\text{Si}(n,\gamma)$  cross section between the two experiments is unknown.

A new measurement of these reactions is of high importance for astrophysical studies. First of all, the bulk of the  $^{29}\text{Si}$  and  $^{30}\text{Si}$  present today in the Milky Way and in the Sun are mostly made in the convective carbon-shell in massive stars at about 1 billion kelvin, and ejected by the supernova explosion [5, 6, 7, 8]. In these stellar conditions, the  $^{28,29,30}\text{Si}$  neutron capture cross sections are crucial to shape the final yields and the relative abundances of  $^{29}\text{Si}$  and  $^{30}\text{Si}$  (see Fig. 1).

However, the relevance of these cross sections is not only limited to galactic chemical evolution and the origin of the Si isotopes in stars. Accurate cross section data are crucial for understanding the isotopic abundances of presolar grains. Presolar stardust grains are tiny inclusions found in meteorites which condensed from outflowing gasses of stellar winds and stellar explosions, shortly before the formation of the solar system [9, 10]. The unique isotopic abundance signatures of these grains can offer clues of their astrophysical origin, and they are essential to study stellar processes and improve the modelling of stellar evolution [11, 12, 13]. Presolar SiC grains of type Mainstream, type Y and type Z are made in low-mass Asymptotic Giant Branch (AGB) stars [9, 14, 15, 16]. In these stars, carbon freshly synthesized in the interior is dredged up to the surface and ejected through stellar winds. Then, SiC grains can form within the circumstellar envelope of these stars and their Si isotopic abundances reflect the signature of the internal neutron-capture nucleosynthesis superimposed on the composition of the pre-stellar gas, as modeled by the galactic chemical evolution. For these grains, isotopic silicon ratios have been accurately measured in the laboratory, with uncertainties lower than 5% (see, e.g., [17]). A precise knowledge of neutron-capture cross sections on the stable silicon isotopes is of paramount importance to disentangle the intrinsic stellar contribution from that of galactic chemical evolution. According to their analysis, comparing the Si abundances of presolar SiC grains of Type Y and Z to AGB models, Zinner et al. [17] favoured the value proposed by Guber et al. [1]. A new measurement of the Si isotope cross sections and in particular of the mysterious  $^{30}\text{Si}(n,\gamma)$  is crucial to confirm those results.

SiC grains of type X and C likely originate from core-collapse supernovae [18, 19, 9]. Those belonging to the rare type C sub-group show peculiar abundances of Si and S isotopes. In particular, Pignatari et al. [19] showed that the strongly enhanced abundance of  $^{32}\text{S}$

S 29 187 ms $\beta^+$ $\gamma$ 1384... $\beta p$ 5.44; 2.13...	S 30 1.18 s $\beta^+$ 4.4; 5.1... $\gamma$ 678...	S 31 2.58 s $\beta^+$ 4.4... $\gamma$ 1266...	S 32 94.99 $\sigma$ 0.55 $\sigma_{n,\alpha} < 0.0005$	S 33 0.75 $\sigma$ 0.46 $\sigma_{n,\alpha}$ 0.12 $\sigma_{n,p}$ 0.002	S 34 4.25 $\sigma$ 0.25	S 35 27.5 d $\beta^-$ 0.2 no $\gamma$	S 36 0.01 $\sigma$ 0.24
P 28 268 ms $\beta^+$ 11.5... $\gamma$ 1779; 4497... $\beta p$ 0.680; 0.956... $\beta n$ 2.105; 1.434...	P 29 4.1 s $\beta^+$ 3.9... $\gamma$ 1273...	P 30 2.50 m $\beta^+$ 3.2... $\gamma$ (2235...)	P 31 100 $\sigma$ 0.17	P 32 14.26 d $\beta^-$ 1.7 no $\gamma$	P 33 25.34 d $\beta^-$ 0.2 no $\gamma$	P 34 12.4 s $\beta^-$ 5.4... $\gamma$ 2127...	P 35 47.4 s $\beta^-$ 2.3... $\gamma$ 1572...
Si 27 4.16 s $\beta^+$ 3.8... $\gamma$ (2210...)	Si 28 92.223 $\sigma$ 0.17	Si 29 4.685 $\sigma$ 0.12	Si 30 3.092 $\sigma$ 0.107	Si 31 2.62 h $\beta^-$ 1.5... $\gamma$ (1266) $\sigma$ 0.073	Si 32 172 a $\beta^-$ 0.2 no $\gamma$ $\sigma < 0.5$	Si 33 6.18 s $\beta^-$ 3.9; 5.8... $\gamma$ 1848...	Si 34 2.77 s $\beta^-$ 3.1 $\gamma$ 1179; 429; 1608
Al 26 6.35 s $\beta^+$ 3.2 $\gamma$ 1130... $\sigma_{n,p}$ 0.34 $\sigma_{n,\alpha}$ 1.97	Al 27 100 $\sigma$ 0.230	Al 28 2.246 m $\beta^-$ 2.9 $\gamma$ 1779	Al 29 6.6 m $\beta^-$ 2.5... $\gamma$ 1273; 2426; 2028...	Al 30 3.60 s $\beta^-$ 5.1; 6.3... $\gamma$ 2235; 1263; 3498...	Al 31 644 ms $\beta^-$ 5.6; 7.9... $\gamma$ 2317; 1695...	Al 32 33 ms $\beta^-$ $\gamma$ 1941; 3042; 4230...	Al 33 41.7 ms $\beta^-$ Bn $\gamma$ 1941*; 4341; 1010

Figure 1: s-process flow in the mass region of interest for the measurement.

can only be explained by the presence of the long-lived  $^{32}\text{Si}$  ( $t_{1/2} = 132$  yr) in the ejecta, produced by neutron capture processes starting from the stable Si isotopes.  $^{32}\text{S}$  is the stable radiogenic product of  $^{32}\text{Si}$  and is not directly implanted in the grains. However, the neutron density has to be high enough to overcome the rather short-lived  $^{31}\text{Si}$  ( $t_{1/2} = 2.6$  hr). The abundance of  $^{32}\text{S}$  in the grains can therefore provide constraints on the neutron density reached during the SN explosion in the C-rich He shell material. All the neutron capture cross sections along the chain of Si isotopes (see Fig. 1) are an essential input in nucleosynthesis calculations to explain presolar grain abundances [19].

Finally, a detailed knowledge of silicon neutron capture rates is fundamental to properly compare theoretical silicon isotopic ratios with SiO maser radio observations of OH/IR stars, commonly linked to intermediate mass AGB stars ( $M > 5 M_{\odot}$ ).

## 2 Experimental Setup

We propose to accurately measure  $^{28,29,30}\text{Si}(n,\gamma)$  cross sections at n\_TOF EAR-1 and EAR-2. At EAR-1, we will take advantage of the excellent neutron energy resolution and high instantaneous neutron flux, allowing a measurement up to a few hundred keV neutron energy. At EAR-2, we plan to measure the cross section at thermal neutron energies (25.3 meV), and the excitation function of the cross section at low energy. Such a study is not possible at EAR-1, due to uncertainties in the neutron beam profile at very low energy, where gravity effects play a role. In addition, the thermal neutron flux in EAR-1 is strongly suppressed by the borated water moderator and, therefore, a measurement of the thermal cross section is much less efficient compared to EAR-2. In both areas, we plan to detect the prompt  $\gamma$  radiation following a capture event using the well-established  $\text{C}_6\text{D}_6$  detection system, consisting of 4 Legnaro type  $\text{C}_6\text{D}_6$  detectors which have been specifically optimised for low neutron sensitivity [20]. In addition, we will complement the  $\text{C}_6\text{D}_6$  detectors at EAR-2 with sTED detectors to measure the 4.9

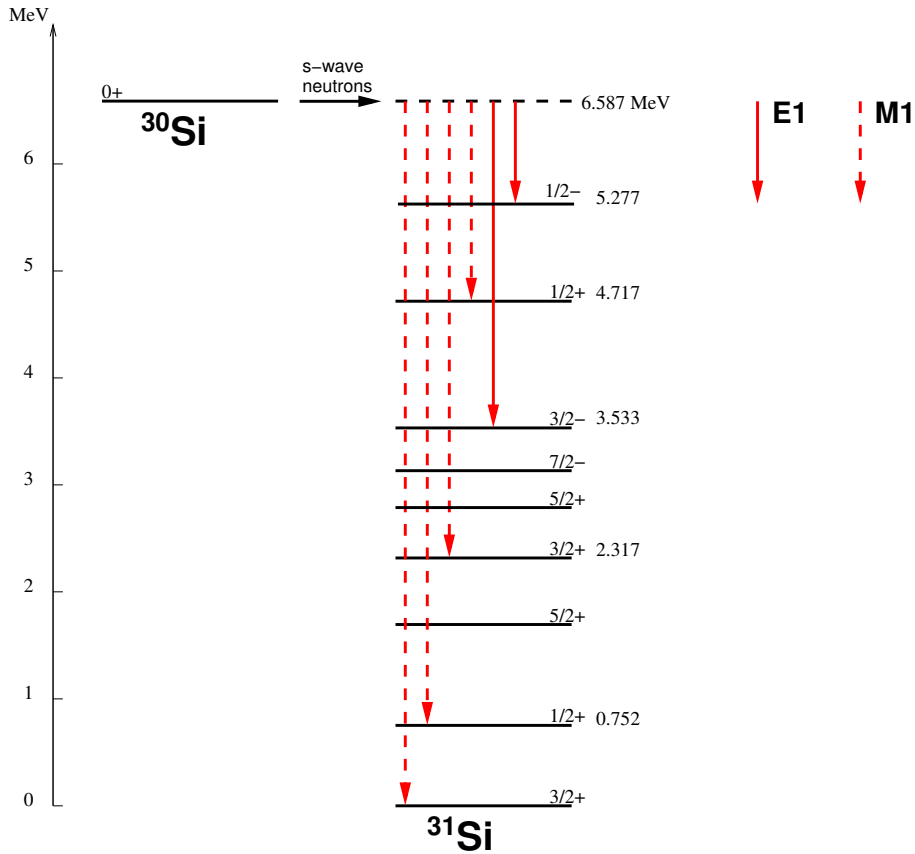


Figure 2: Primary  $\gamma$ -rays emitted following neutron capture events by  $^{30}\text{Si}$ .

eV resonance in Au, since for this type of detector dead-time-corrections will be smaller, and as a consequence, a reliable normalisation to obtain absolute cross section values can be obtained. An example of the expected primary  $\gamma$ -rays emitted by s-wave neutrons capture by  $^{31}\text{Si}$  is shown in Figure 2. Additional  $\gamma$ 's are expected, obviously, from the decay cascade.

Each of the Si samples will consist of 1g of enriched (all three over 99%) metal, in form of a cylindrical disc of 2 cm diameter. Similar to other capture experiments, the data will be normalised using the saturated resonance technique on Au, measuring a Au sample of the same diameter as the Si samples. Backgrounds will be determined in runs with an empty sample holder, and the neutron scattering background will be studied by measuring with a natural Carbon sample.

For all silicon isotopes, the stellar cross section is determined by only very few resonances. This implies that these resonances need to be studied with high accuracy, due to their high impact on the stellar cross section. In addition, the direct capture component could play a significant role (details provided in [21]).

For our count rate estimates, we have taken into consideration the most recent evaluation of the neutron flux at EAR-1, the resolution function, and the cross sections available

from the ENDF/B-VIII evaluation. For  $^{30}\text{Si}$ , the first resonance at 2.235 keV has been removed as the presence of this resonance has been questioned and its non-existence confirmed in preliminary data taken with a natural-Si sample measured at n\_TOF in 2021, during the commissioning. For the background estimation, we have taken data from a previous measurement with a similar setup. The panels to the left in Figure 3 show the count rate estimation with the assumptions described above for all three stable Si isotopes, assuming  $2 \times 10^{18}$  protons on target each. Only the resonant energy region is shown in the Figure. All resonances of interest are well resolved and have good counting statistics, as indicated by the star symbol which shows the total number of counts in each resonance. For background and normalisation measurements, we request  $1 \times 10^{18}$  protons. This will allow us to determine the background accurately between resonances, which may indicate if there is a strong, direct p-wave contribution to the cross section and high neutron energy.

Due to the 30 times higher neutron flux, we only require a modest amount of beam time for the EAR-2 measurement,  $2 \times 10^{17}$  protons per isotope. The right column of Figure 3 shows the expected count rate at low energy for each isotope. We have also included the expected background for this measurement due to reactions of neutrons in the experimental area (data from a recent capture measurement on Mo isotopes). The cross section at EAR-2 can be measured up to a few eV, which will provide important information on the contribution of sub-threshold resonances or the direct capture component. For normalisation and background studies, we request a further  $5 \times 10^{17}$  protons on target.

**Summary of requested protons:**  $7 \times 10^{18}$  protons EAR-1,  $1.1 \times 10^{18}$  at EAR-2 (can be split over 2 years)

## References

- [1] K.H. Guber, P.E. Koehler, H. Derrien, T.E. Valentine, L.C. Leal, R.O. Sayer, and T. Rauscher. *Phys. Rev. C*, 67:062802, 2003.
- [2] J. W. Boldeman, B. J. Allen, A. R. de L. Musgrove, and R. L. Macklin. The neutron capture cross section of natural silicon. *Nuclear Physics A*, 252(1):62–76, November 1975.
- [3] M. J. Kenny, B. J. Allen, J. W. Boldeman, and A. M. R. Joye. Resonance neutron capture in silicon. *Nuclear Physics A*, 270(1):164–174, October 1976.
- [4] H. Beer, P.V. Sedyshev, W. Rochow, T. Rauscher, and P. Mohr. *Nucl. Phys. A*, 453:062802, 2002.
- [5] S. E. Woosley and Thomas A. Weaver. The Evolution and Explosion of Massive Stars. II. Explosive Hydrodynamics and Nucleosynthesis. *The Astrophysical Journal Supplement Series*, 101:181, November 1995.
- [6] A. Chieffi, M. Limongi, and O. Straniero. The Evolution of a  $25 M_{\odot}$  Star from the Main Sequence up to the Onset of the Iron Core Collapse. *The Astrophysical Journal*, 502(2):737–762, August 1998.

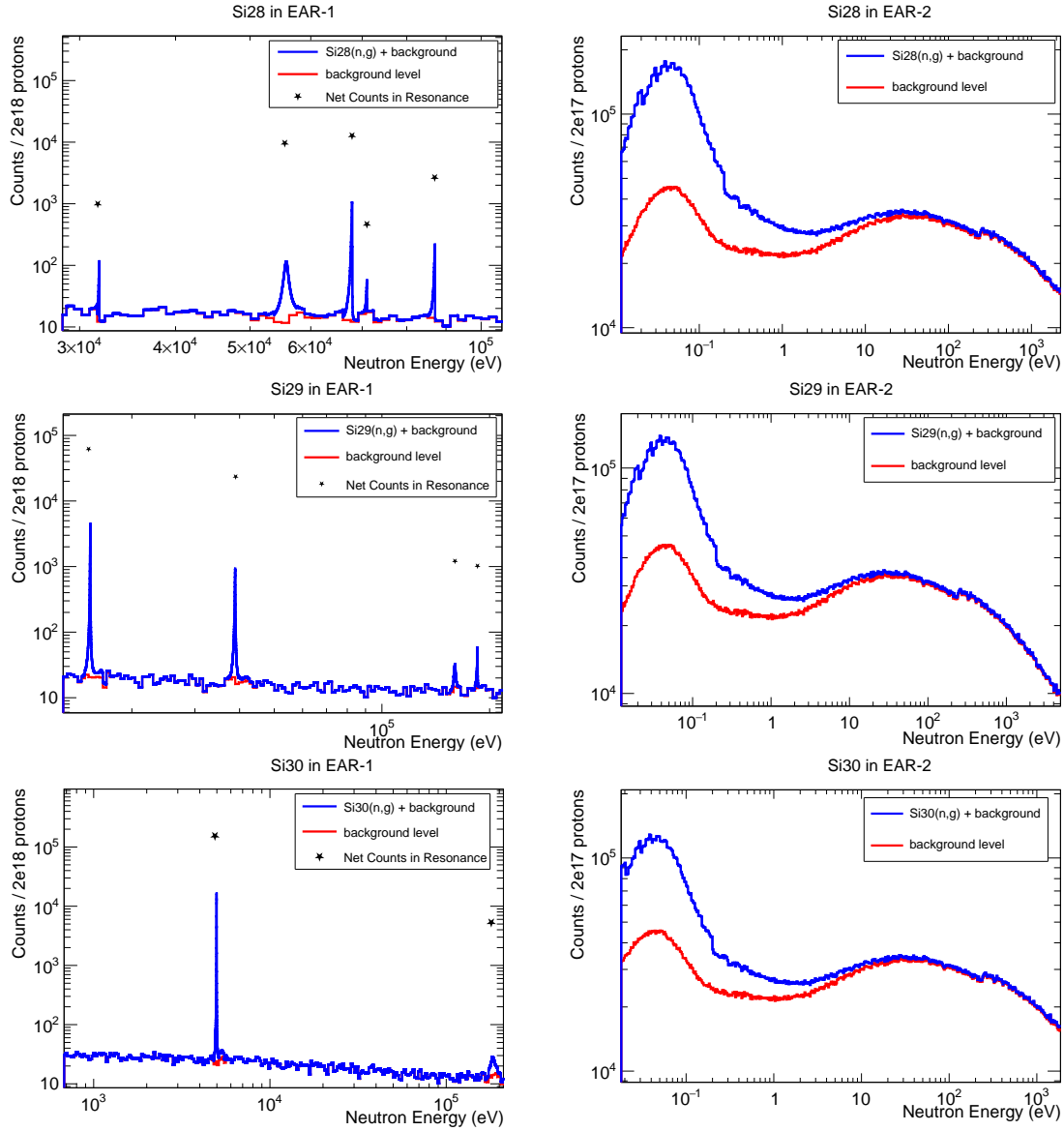


Figure 3: (Panels to the left) Count rate estimate for each of the stable Si isotopes for  $2 \times 10^{18}$  protons on target in EAR-1. The number of counts expected in each resonance is shown by a star symbol. (Panels to the right) Count rate estimate for each of the stable Si isotopes for  $2 \times 10^{17}$  protons on target in EAR-2. For both experimental areas, the background level has been estimated from previous measurements.

- [7] S. E. Woosley, A. Heger, and T. A. Weaver. The evolution and explosion of massive stars. *Reviews of Modern Physics*, 74(4):1015–1071, November 2002.
- [8] M. Pignatari, F. Herwig, R. Hirschi, M. Bennett, G. Rockefeller, C. Fryer, F. X. Timmes, C. Ritter, A. Heger, S. Jones, U. Battino, A. Dotter, R. Trappitsch, S. Diehl, U. Frischknecht, A. Hungerford, G. Magkotsios, C. Travaglio, and P. Young. NuGrid Stellar Data Set. I. Stellar Yields from H to Bi for Stars with Metallicities  $Z = 0.02$  and  $Z = 0.01$ . *The Astrophysical Journal Supplement Series*, 225(2):24, August 2016.
- [9] E. Zinner. Presolar Grains. In Andrew M. Davis, editor, *Meteorites and Cosmochemical Processes*, volume 1, pages 181–213. 2014.
- [10] L. R. Nittler and F. Ciesla. Astrophysics with Extraterrestrial Materials. *Annual Review of Astronomy and Astrophysics*, 54:53–93, September 2016.
- [11] C. Travaglio, R. Gallino, S. Amari, E. Zinner, S. Woosley, and R. S. Lewis. Low-Density Graphite Grains and Mixing in Type II Supernovae. *The Astrophysical Journal*, 510(1):325–354, January 1999.
- [12] M. Lugaro, A. M. Davis, R. Gallino, M. J. Pellin, O. Straniero, and F. Käppeler. Isotopic Compositions of Strontium, Zirconium, Molybdenum, and Barium in Single Presolar SiC Grains and Asymptotic Giant Branch Stars. *The Astrophysical Journal*, 593(1):486–508, August 2003.
- [13] M. Pignatari, E. Zinner, P. Hoppe, C. J. Jordan, B. K. Gibson, R. Trappitsch, F. Herwig, C. Fryer, R. Hirschi, and F. X. Timmes. Carbon-rich Presolar Grains from Massive Stars: Subsolar  $^{12}\text{C}/^{13}\text{C}$  and  $^{14}\text{N}/^{15}\text{N}$  Ratios and the Mystery of  $^{15}\text{N}$ . *Astrophysical Journal Letters*, 808(2):L43, August 2015.
- [14] M. Lugaro, B. Cseh, B. Világos, A. I. Karakas, P. Ventura, F. Dell’Agli, R. Trappitsch, M. Hampel, V. D’Orazi, C. B. Pereira, G. Tagliente, G. M. Szabó, M. Pignatari, U. Battino, A. Tattersall, M. Ek, M. Schönabächler, J. Hron, and L. R. Nittler. Origin of Large Meteoritic SiC Stardust Grains in Metal-rich AGB Stars. *The Astrophysical Journal*, 898(2):96, August 2020.
- [15] S. Cristallo, A. Nanni, G. Cescutti, I. Minchev, N. Liu, D. Vescovi, D. Gobrecht, and L. Piersanti. Mass and metallicity distribution of parent agb stars of presolar sic. *Astronomy & Astrophysics*, 644:A8, December 2020.
- [16] S. Palmerini, M. Busso, D. Vescovi, E. Naselli, A. Piatella, R. Mucciola, S. Cristallo, D. Mascalì, A. Mengoni, S. Simonucci, and S. Taioli. Presolar Grain Isotopic Ratios as Constraints to Nuclear and Stellar Parameters of Asymptotic Giant Branch Star Nucleosynthesis. *The Astrophysical Journal*, 921(1):7, November 2021.
- [17] Ernst Zinner, Larry R. Nittler, Roberto Gallino, Amanda I. Karakas, Maria Lugaro, Oscar Straniero, and John C. Lattanzio. Silicon and Carbon Isotopic Ratios in AGB Stars: SiC Grain Data, Models, and the Galactic Evolution of the Si Isotopes. *The Astrophysical Journal*, 650(1):350–373, October 2006.

- [18] Peter Hoppe, Wataru Fujiya, and Ernst Zinner. Sulfur molecule chemistry in supernova ejecta recorded by silicon carbide stardust. *The Astrophysical Journal Letters*, 745(2):L26, jan 2012.
- [19] M. Pignatari, E. Zinner, M. G. Bertolli, R. Trappitsch, P. Hoppe, T. Rauscher, C. Fryer, F. Herwig, R. Hirschi, F. X. Timmes, and F. K. Thielemann. Silicon Carbide Grains of Type C Provide Evidence for the Production of the Unstable Isotope  $^{32}\text{Si}$  in Supernovae. *he Astrophysical Journal Letters*, 771(1):L7, July 2013.
- [20] Pierfrancesco Mastinu, Roberto Baccomi, Eric Berthoumieux, Daniel Cano-Ott, F Gramegna, Carlos Guerrero, Cristian Massimi, Paolo Maria Milazzo, Federica Mingrone, Javier Praena, G Prete, and Aczel Regino García. New  $\text{C}_6\text{D}_6$  detectors: reduced neutron sensitivity and improved safety. 2013.
- [21] A. Mengoni. *See the twiki page*, 2023.



# Appendix

## DESCRIPTION OF THE PROPOSED EXPERIMENT

Please describe here below the main parts of your experimental set-up:

Part of the experiment	Design and manufacturing
If relevant, write here the name of the <u>fixed</u> installation you will be using [C6D6 detectors]	<input checked="" type="checkbox"/> To be used without any modification <input type="checkbox"/> To be modified
If relevant, write here the name of the <u>fixed</u> installation you will be using [Si-Mon]	<input checked="" type="checkbox"/> To be used without any modification <input type="checkbox"/> To be modified
If relevant, write here the name of the <u>fixed</u> installation you will be using [sTED]	<input checked="" type="checkbox"/> To be used without any modification <input type="checkbox"/> To be modified
If relevant, describe here the name of the <u>flexible/transported</u> equipment you will bring to CERN from your Institute []	<input type="checkbox"/> Standard equipment supplied by a manufacturer <input type="checkbox"/> CERN/collaboration responsible for the design and/or manufacturing
Small spare parts, such as detector holders, cabling, spare detectors etc.	<input checked="" type="checkbox"/> Standard equipment supplied by a manufacturer <input checked="" type="checkbox"/> CERN/collaboration responsible for the design and/or manufacturing
[insert lines if needed]	

## HAZARDS GENERATED BY THE EXPERIMENT

Additional hazard from flexible or transported equipment to the CERN site:

Domain	Hazards/Hazardous Activities	Description
Mechanical Safety	Pressure	<input type="checkbox"/> [pressure] [bar], [volume][l]
	Vacuum	<input type="checkbox"/>
	Machine tools	<input type="checkbox"/>
	Mechanical energy (moving parts)	<input type="checkbox"/>
	Hot/Cold surfaces	<input type="checkbox"/>
Cryogenic Safety	Cryogenic fluid	<input type="checkbox"/> [fluid] [m3]
Electrical Safety	Electrical equipment and installations	<input type="checkbox"/> [voltage] [V], [current] [A]
	High Voltage equipment	<input type="checkbox"/> [voltage] [V]
Chemical Safety	CMR (carcinogens, mutagens and toxic to reproduction)	<input type="checkbox"/> [fluid], [quantity]
	Toxic/Irritant	<input type="checkbox"/> [fluid], [quantity]
	Corrosive	<input type="checkbox"/> [fluid], [quantity]
	Oxidizing	<input type="checkbox"/> [fluid], [quantity]

	Flammable/Potentially explosive atmospheres	<input type="checkbox"/>	[fluid], [quantity]
	Dangerous for the environment	<input type="checkbox"/>	[fluid], [quantity]
Non-ionizing radiation Safety	Laser	<input type="checkbox"/>	[laser], [class]
	UV light	<input type="checkbox"/>	
	Magnetic field	<input type="checkbox"/>	[magnetic field] [T]
Workplace	Excessive noise	<input type="checkbox"/>	
	Working outside normal working hours	<input type="checkbox"/>	
	Working at height (climbing platforms, etc.)	<input type="checkbox"/>	
	Outdoor activities	<input type="checkbox"/>	
Fire Safety	Ignition sources	<input type="checkbox"/>	
	Combustible Materials	<input type="checkbox"/>	
	Hot Work (e.g. welding, grinding)	<input type="checkbox"/>	
Other hazards			